

Electrochemical crystallization and functional properties of nickel-based composite coatings

V.N. Tseluikin , A.S. Dzhumieva , A.I. Tribis , D.A. Tikhonov 

Yuri Gagarin State Technical University or Saratov, Saratov, Russian Federation

✉ tseluikin@mail.ru

ABSTRACT

The electrochemical crystallization of nickel/graphene oxide composite electrochemical coatings was researched by the chronovoltamperometry method. The microstructure of the composite electrochemical coatings was studied by scanning electron microscopy and X-ray diffraction analysis. The microhardness and corrosion rate of nickel/graphene oxide composite electrochemical coatings obtained at different cathode current densities were measured. It was revealed that in the presence of a dispersed phase of multilayer graphene oxide, the rate of the cathode process increases. Based on scanning electron microscopy and X-ray diffraction data, it was found that the dispersed phase affects the crystal structure of the nickel matrix. In the presence of graphene oxide, the nickel deposit is formed uniform and fine-grained. It was found that the microhardness of the nickel/graphene oxide composite electrochemical coatings increases ~ 1.20 times compared with pure nickel. This is a consequence of the formation of fine crystalline deposits with long grain boundaries, which prevents the movement of dislocations and plastic deformation of the crystal lattice. Tests in 3.5% NaCl showed that the inclusion of graphene oxide particles in the composition of electrolytic nickel deposits leads to a decrease in their corrosion rate by 1.35–1.60 times. This effect is due to the fact that graphene oxide particles ensure a uniform distribution of corrosion currents over the coating surface, and in the structure of composite electrochemical coatings, the dispersed phase forms compounds that are more corrosion resistant than the metal matrix.

KEYWORDS

electrochemical composition coatings • nickel • graphene oxide • microhardness • corrosion

Citation: Tseluikin VN, Dzhumieva AS, Tribis AI, Tikhonov DA. Electrochemical crystallization and functional properties of nickel-based composite coatings. *Materials Physics and Mechanics*. 2025;53(2): 142–148.

http://dx.doi.org/10.18149/MPM.5322025_12

Introduction

Electrochemical deposition of coatings based on nickel and its alloys is one of the most effective methods for surface modification of steel products to protect them against wear and corrosion [1]. Significant improvement in the characteristics of electrolytic nickel can be achieved through its co-deposition with various dispersed particles. Electrochemical deposits modified with a dispersed phase are called composite electrochemical coatings (CECs). In particular, nickel-based CECs, due to their excellent adhesion, high hardness and abrasion resistance, find applications in mechanical engineering, chemical and oil/gas industries, medical equipment etc. [2–4].

The performance characteristics of composite coatings are largely determined by the dispersed phase. Among the wide variety of dispersed materials, carbon derivatives have attracted considerable attention from researchers. Specifically, nickel CECs modified with carbon nanotubes [5–7], fullerenes [8,9], nanodiamonds [10,11], graphene and its oxide [12–16] have been obtained. The latter occupies a special place among carbon



compounds. Graphene is a two-dimensional material with a high specific surface area. Its interaction with strong mineral acids leads to the formation of graphene oxide (GO). In the structure of GO, carbon atoms are bonded to oxide functional groups (carbonyl, carboxyl, epoxy etc.), which make it hydrophilic and enable the formation of stable aqueous dispersions. These compounds are inert in many aggressive environments, making them suitable for corrosion protection [17–19]. Additionally, the high physical and mechanical properties of GO are of particular interest [20].

The aim of the present work is to obtain, under stationary electrolysis conditions (galvanostatic mode), composite coatings based on nickel modified with multilayer GO, and to study their structure, physical and mechanical and corrosion properties.

Materials and Methods

The Ni-GO composite coatings were deposited on a steel substrate (Steel 45) from a sulfate-chloride electrolyte (Table 1) with constant stirring using a magnetic stirrer. Pure nickel electrochemical deposits were obtained from a similar solution without the GO dispersed phase. The coating thickness was 20 μm . Preliminary preparation of the electrode surface prior to coating deposition included mechanical polishing with micron-grade sandpaper, anodic treatment in 48 % H_3PO_4 at a current density of 50 A/dm^2 for 5 sec and rinsing with distilled water.

Table 1. Electrolyte composition and electrochemical deposition parameters

No.	Electrolyte composition	Concentration, g/l	Deposition parameters
1	$\text{NiSO}_4 \cdot 7\text{H}_2\text{O}$	220	Temperature $T = 45\text{ }^\circ\text{C}$ Cathode current density $i_k = 7, 8, 9, 10\text{ A}/\text{dm}^2$
2	$\text{NiCl}_2 \cdot 6\text{H}_2\text{O}$	40	
3	CH_3COONa	30	
4	graphene oxide	10	

Multilayer GO was synthesized through electrochemical oxidation of natural graphite powder GB/T 3518-95 (China) in galvanostatic mode. A detailed description of the synthesis method and the structure of the formed GO is provided in [21]. Phase composition studies were conducted using an ARL X'TRA device (Thermo Scientific, Ecublens, Switzerland) with Cu $K\alpha$ radiation ($\lambda = 0.15412\text{ nm}$). The surface morphology of nickel coatings was examined using an ASPEX Explorer scanning electron microscope (ASPEX, Framingham, MA, USA). Electrochemical measurements were performed using a P-30J potentiostat (Elins LLC, Russia). Potentials were set relative to a saturated silver/chloride reference electrode and recalculated according to the hydrogen scale.

The Vickers microhardness (HV) of the deposits was measured using a PMT-3 instrument (LOMO JSC, Russia) by static indentation of a diamond pyramid under a 100 g load. HV values were calculated based on seven parallel tests, with a measurement error of 3 %. The surface roughness parameter (R_a) of nickel coatings was determined using a TR 220 profilograph-profilometer (TIME GROUP Inc., China). The average roughness value was calculated from five parallel measurements. To evaluate the corrosion rate of nickel coatings, studies were conducted in a 3.5 % NaCl solution.

Results and Discussion

During electrochemical co-deposition with metals, dispersed phase particles influence the kinetics of electrode (cathodic) processes. As chronovoltamperometry results show (Fig. 1), nickel electrodeposition in the presence of GO exhibits a potential shift toward more positive values compared to pure nickel. Consequently, the cathodic reduction rate increases for Ni-GO CECs. Morphological analysis of GO revealed [21] that this compound has an ordered layered structure with individual layer thickness below 0.1 μm . The Brunauer–Emmett–Teller method determined GO's specific surface area as 46.78 m^2/g [21]. The developed surface of GO may adsorb cations from the solution, leading to positive charging of dispersed phase particles. Therefore, GO transfer to the cathode occurs not only through convection, but also via electrophoretic forces [14–16].

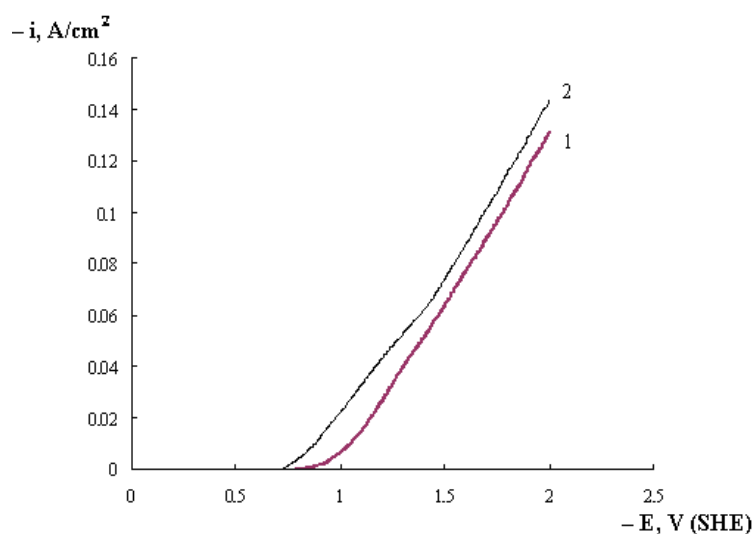


Fig. 1. Potentiodynamic polarization curves of electrochemical deposition of nickel (1) and CEC Ni-GO (2) (potential sweep rate $V_p = 8 \text{ mV/s}$)

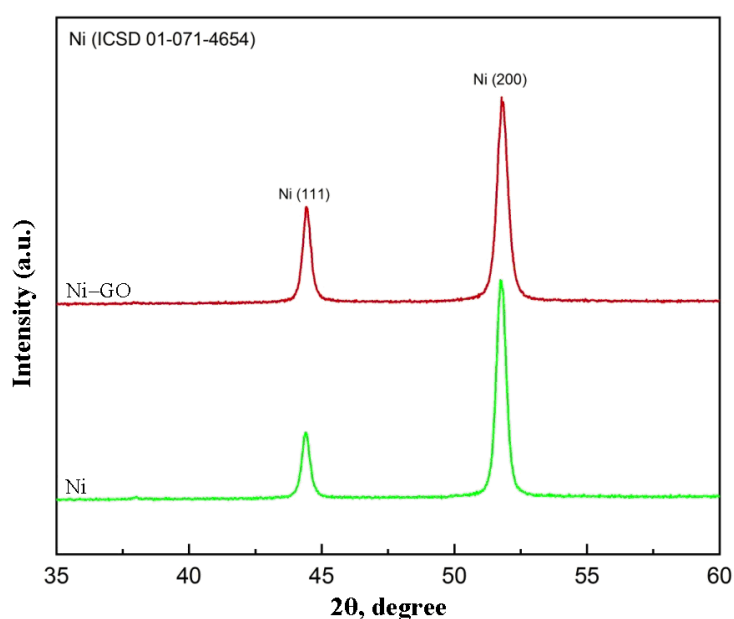


Fig. 2. XRD pattern of nickel and Ni-GO CEC obtained at a current density of $i_k = 10 \text{ A}/\text{dm}^2$

X-ray diffraction analysis (XRD) of the obtained coatings revealed changes in nickel's crystal structure under GO influence. X-ray diffraction peaks at 44.5° and 52.2° (Fig. 2) correspond to nickel's (111) and (200) crystal planes, respectively [11]. According to the X-ray diffraction, the main orientation for nickel crystals is the (200) direction. While peak intensities at 52.2° remain unchanged for nickel without dispersed phase and Ni-GO CECs, GO presence increases the 44.5° peak intensity, indicating enhanced crystal growth along the (111) plane. Clearly, the dispersed phase affects the nickel matrix's crystalline structure. GO layers may serve as nucleation sites for metal deposits, restricting grain growth and making them more compact.

Scanning electron microscopy (SEM) analysis of nickel coatings' surface morphology demonstrated GO's structural influence. Electrolytic nickel without dispersed phase (Fig. 3(a)) shows disordered, coarse-grained structure approaching X-ray amorphous state. With GO present, ordered, fine-grained and uniform nickel deposits form (Fig. 3(b)). SEM analysis of the composite coatings confirmed carbon presence, proving GO incorporation into the nickel matrix.

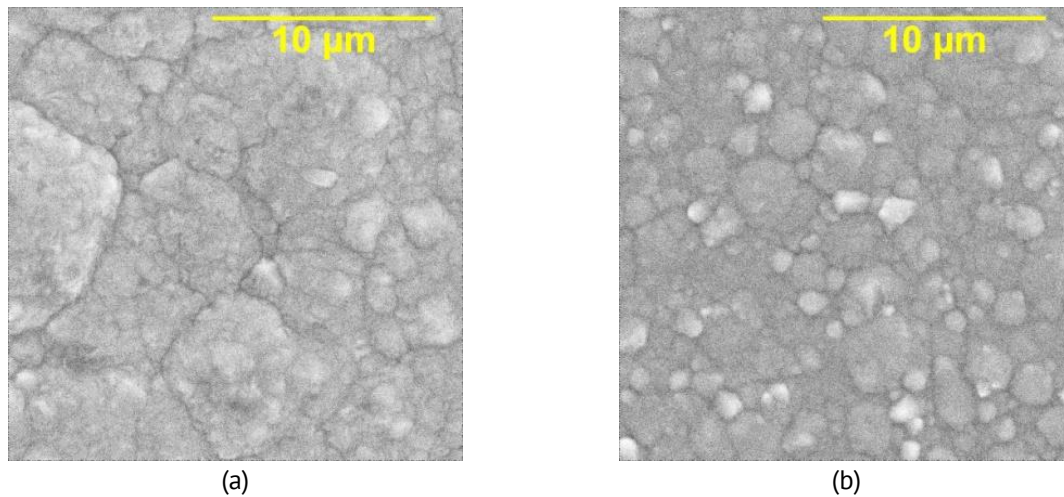


Fig. 3. SEM images of the nickel surface (a) and the Ni-GO composite coating (b) obtained at a cathode current density of $i_k = 10 \text{ A/dm}^2$. Magnification $\times 10000$

Grain size calculations based on XPA data (Fig. 2) at the intensity of the crystal lattice (111) using Scherrer's equation [22]: $d = \frac{0.9\lambda}{b \cos \theta}$, where λ is the wave length and equals 0.15412 nm, b is the peak width at half maximum, θ is the diffraction angle. The calculations revealed grain size reduction from 69.0 nm (nickel without dispersed phase) to 21.5 nm (Ni-GO CEC), i.e., over threefold decrease.

Table 2. Parameter R_a values, μm of surface roughness of nickel-based coatings

Cathode current density i_k , A/dm^2	Roughness parameter R_a , μm	
	Nickel	Ni-GO
7	1.395	0.673
8	1.017	0.420
9	0.771	0.401
10	0.596	0.369

To characterize the electrolytic nickel deposits condition, its surface roughness was measured, i.e., arithmetic mean of absolute values of profile deviations within the base length (R_a). The R_a parameter values decrease for composite coatings across studied current densities compared with pure nickel (Table 2). Evidently, GO particles promote uniform metal deposit distribution across the cathode surface without causing agglomeration in the nickel matrix volume.

The reduction in grain size of nickel deposits and the associated change in surface morphology should affect their physical and mechanical properties. The GO layers within the coating volume act as vacancy sites and inhibit metal grain growth. This process leads to an increased nucleation rate. The crystallites become finer, and the extended grain boundaries impede dislocation movement and plastic deformation of the crystal lattice [11]. Notably, GO possesses high mechanical properties. When an external load is applied to the composite coating, the GO layers absorb part of the load through shear stress transfer. Dislocation motion in the nickel matrix is constrained by the GO particle layers, resulting in deformation resistance and increased lattice distortion energy [23,24]. These factors enhance microhardness from 1938–2459 MPa (nickel without dispersed phase) to 2200–3076 MPa (Ni-GO CEC), i.e., by ~ 20 % (Table 3). The microhardness of the Steel 45 substrate was 894 MPa.

Table 3. Microhardness values HV_{100} of nickel-based coatings

Cathode current density i_k , A/dm ²	Microhardness HV_{100} , MPa	
	Nickel	Ni-GO
7	1938	2200
8	2150	2520
9	2350	2938
10	2459	3076

Another critical operational property of composite coatings is corrosion resistance. The corrosion rate (CR) of nickel deposits was determined by mass loss after 24-hour immersion in 3.5 % NaCl (weighing before/after testing) using the following equation [25,26]: $CR = \frac{KW}{AtD}$, where K is the constant ($8.76 \cdot 10^4$), W is the mass loss (g), A is the coating area (1 cm²), t is the testing time (h) and D is the nickel density, which equals 8.9 g/sm³. Corrosion tests in 3.5 % NaCl revealed a decrease in corrosion rate from 0.328–0.656 mm/year (nickel without dispersed phase) to 0.205–0.492 mm/year (Ni-GO CEC), i.e., ~40% reduction (Table 4). The Steel 45 substrate exhibited a corrosion rate of 0.881 mm/year.

Table 4. Corrosion rate of nickel-based coatings









Cathode current density i_k , A/dm ²	Corrosion rate, mm/year	
	Nickel	Ni-GO
7	0.656	0.492
8	0.574	0.410
9	0.451	0.328
10	0.328	0.205

The primary factors governing corrosion behavior of the electrolytic nickel deposits are its composition and structure. Nickel's electrochemical corrosion susceptibility depends on crystallographic orientation, which determines surface free energy per unit area [25]. The ordered fine-crystalline structure of CECs (Fig. 3(b)), unlike nickel without dispersed phase (Fig. 3(a)), promotes uniform corrosion current distribution [27,28]. Dispersed phase agglomeration in the metal matrix worsens corrosion properties by forming microgalvanic elements [29]. Thus, GO inclusions are uniformly distributed throughout the coating volume and surface. Moreover, GO's stability and impermeability elongates the diffusion path for aggressive media [30], preventing nickel ion penetration through GO particle cross-sections. It is worth noting that the dispersed phase enhances corrosion resistance only if it forms compounds more stable than the metal matrix at phase boundaries or throughout the whole volume. Otherwise, corrosion won't stop, bypassing the particles (with possible minor rate reduction). Such stable compounds evidently form in the studied Ni-GO CEC structure. All the factors listed above improve the corrosion resistance of Ni-GO CECs compared to pure nickel deposits.

Conclusions

The conducted studies allow to conclude that in the galvanostatic electrolysis mode from a sulfate-chloride nickel-plating electrolyte containing a dispersion of multilayer GO, composite coatings are formed. The incorporation of the GO phase into the matrix of electrolytic nickel deposits leads to changes in their surface microtopography and a reduction in grain size from 69 to 21.5 nm. GO contributes to the improvement of physical and mechanical and corrosion properties of the studied CECs. Modification of the electrochemical coating with dispersed particles results in an increase of microhardness from 1938–2459 to 2200–3076 MPa, as well as a decrease in corrosion rate from 0.328–0.656 mm/year for nickel without dispersed phase to 0.205–0.492 mm/year for Ni-GO CECs.

CRedit authorship contribution statement

Vitaly N. Tseluikin  : supervision, conceptualization, writing – review & editing, writing – original draft; **Asel S. Dzhumieva**  : investigation, data curation, writing – review & editing; **Alena I. Tribis**  : investigation, data curation; **Denis A. Tikhonov**  : investigation, data curation.

Conflict of interest

The authors declare that they have no conflict of interest.

References

1. Orinakova R, Turonova A, Kladekova D, Galova M, Smith RM. Recent developments in the electrodeposition of nickel and some nickel-based alloys. *J. Appl. Electrochem.* 2006;36: 957–972.
2. Low CTJ, Wills RGA, Walsh FC. Electrodeposition of composite coatings containing nanoparticles in a metal deposit. *Surf. Coat. Technol.* 2006;201: 371–383.
3. Walsh FC. A review of the electrodeposition of metal matrix composite coatings by inclusion of particles in a metal layer: An established and diversifying technology. *Trans. IMF.* 2014;92: 83–98.
4. Tseluikin V, Dzhumieva A, Tribis A, Brudnik S, Tikhonov D, Yakovlev A, Mostovoy A, Lopukhova M. Electrochemical Deposition and Properties of Ni Coatings with Nitrogen-Modified Graphene Oxide. *J. Compos. Sci.* 2024;8: 147.

5. Giannopoulos F, Chronopoulou N, Bai J, Zhao H, Pantelis D, Pavlatou EAI, Karatonis A. Nickel/MWCNT-Al₂O₃ electrochemical co-deposition: Structural properties and mechanistics aspects. *Electrochim. Acta*. 2016;207: 76–86.
6. Jyotheender K. S., Gupta A., Srivastava C. Grain boundary engineering in Ni-carbon nanotube composite coatings and its effect on the corrosion behaviour of the coatings. *Materialia*. 2020;9: 100617.
7. Yang P, Wang N, Zhang J, Lei Y, Shu B. Investigation of the microstructure and tribological properties of CNTs/Ni composites prepared by electrodeposition. *Mater. Res. Express*. 2022;9: 036404.
8. Antihovich IV, Ablazhey NM, Chernik AA, Zharsky IM. Electrodeposition of nickel and composite nickel-fullerenol coatings from low-temperature sulphate-chloride-isobutyrate electrolyte. *Procedia Chem*. 2014;10: 373–377.
9. Tseluikin VN. Electrodeposition and properties of composite coatings modified by fullerene C₆₀. *Prot. Met. Phys. Chem. Surf*. 2017;53: 433–436.
10. Chayeuski VV, Zhyllinski VV, Rudak PV, Rusalsky DP, Visniakov N, Cernasejus O. Characteristics of ZrC/Ni-UDD coatings for a tungsten carbide cutting tool. *Appl. Surf. Sci*. 2018;446: 18–26.
11. Makarova I, Dobryden I, Kharitonov D, Kasach A, Ryl J, Repo E, Vuorinen E. Nickel-nanodiamond coatings electrodeposited from tartrate electrolyte at ambient temperature. *Surf. Coat. Technol*. 2019;380: 125063.
12. Algul H, Tokur M, Ozcan S, Uysal M, Cetinkaya T, Akbulut H, Alp A. The effect of graphene content and sliding speed on the wear mechanism of nickel–graphene nanocomposites. *Appl. Surf. Sci*. 2015;359: 340–348.
13. Yasin G, Arif M, Nizam NM, Shakeel M, Khan MA, Khan WQ, Hassan TM, Abbas Z, Farahbakhsh I, Zuo Y. Effect of surfactant concentration in electrolyte on the fabrication and properties of nickel-graphene nanocomposite coating synthesized by electrochemical co-deposition. *RSC Adv*. 2018;8: 20039–20047.
14. Ambrosi A, Pumera M. The structural stability of graphene anticorrosion coating materials is compromised at low potentials. *Chem.-A Eur. J*. 2015;21: 7896–7901.
15. Jyotheender KS, Srivastava C. Ni-graphene oxide composite coatings: Optimum graphene oxide for enhanced corrosion resistance. *Compos. Part B*. 2019;175: 107145.
16. Tseluikin V, Dzhumieva A, Tikhonov D, Yakovlev A, Strilets A, Tribis A, Lopukhova M. Pulsed electrodeposition and properties of nickel-based composite coatings modified with graphene oxide. *Coatings*. 2022;12: 656.
17. Tseluikin V, Dzhumieva A, Yakovlev A, Tikhonov D, Tribis A, Strilets A, Lopukhova M. Electrodeposition and Properties of Composite Ni Coatings Modified with Multilayer Graphene Oxide. *Micromachines*. 2023;14: 1747.
18. Korkmaz S, Kariper IA. Graphene and graphene oxide based aerogels: Synthesis, characteristics and supercapacitor applications. *J. Energy Storage*. 2020;27: 101038.
19. Arvas MB, Gürsu H, Gencten M, Sahin Y. Preparation of different heteroatom doped graphene oxide based electrodes by electrochemical method and their supercapacitor applications. *J. Energy Storage*. 2021;35: 102328.
20. Ropalekar AR, Ghadge RR, Anekar NA. Experimental investigation on flexural fatigue strength of graphene oxide modified E-glass epoxy composite beam. *Materials Physics and Mechanics*. 2024;52(1): 132–141.
21. Yakovlev AV, Yakovleva EV, Vikulova MA, Frolov IN, Rakhmetulina LA, Tseluikin VN, Krasnov VV, Mostovoy AS. Synthesis of multilayer graphene oxide in electrochemical graphite dispersion in H₂SO₄. *Russ. J. Appl. Chem*. 2020;93: 219–224.
22. Zhang H, Zhang N, Fang F. Fabrication of high-performance nickel/graphene oxide composite coatings using ultrasonic assisted. *Ultrason. Sonochem*. 2020;62: 104858.
23. Lai R, Shi P, Yi Z, Li H, Yi Y. Triple-band surface plasmon resonance metamaterial absorber based on open-ended prohibited sign type monolayer graphene. *Micromachines*. 2023;14: 953.
24. Hong Q, Wang D, Yin S. The microstructure, wear and electrochemical properties of electrodeposited Ni-diamond composite coatings: Effect of diamond concentration. *Mat. Tod. Comm*. 2023;34: 105476.
25. Yang F, Kang H, Guo E, Li R, Chen Z, Zeng Y. The role of nickel in mechanical performance and corrosion behaviour of nickel-aluminium bronze in 3.5 wt.% NaCl solution. *Corros. Sci*. 2018; 139: 333–345.
26. Rekha MY, Srivastava C. Microstructural evolution and corrosion behavior of Zn-Ni-graphene oxide composite coatings. *Metall. Mater. Trans. A*. 2019;50: 5896–5913.
27. Wang Y, Tay SL, Wei S, Xiong C, Gao W, Shakoar RA, Kahraman R. Microstructure and properties of sol-enhanced Ni-Co-TiO₂ nano-composite coatings on mild steel. *J. Alloys Compd*. 2015;649: 222–228.
28. Lou G, Shen L, Qian Y, Chen Y, Bai H, Cheng H, Xu J, Yang Y. Study on the antibacterial and anti-corrosion properties of Ni-GO/Ni-rGO composite coating on manganese steel. *Surf. Coat. Technol*. 2021; 424: 127681.
29. Vodopyanova S, Mingazova G, Fomina R, Sayfullin R. Physical and mechanical properties of modified chrome coatings. *Materials Physics and Mechanics*. 2023;51(7): 123–136.
30. Carboni N, Mazzapoda L, Capr A, Gatto I, Carbone A, Baglio V, Navarra MA. Composite Anion Exchange Membranes based on Graphene Oxide for Water Electrolyzer Applications. *Electrochim. Acta*. 2024;486: 144090.